

Polymorphism of Poly(di-*n*-pentylsilane)

E. K. Karikari and B. L. Farmer*

Department of Materials Science and Engineering, University of Virginia, Charlottesville, Virginia 22903-2442

C. L. Hoffmann and J. F. Rabolt

*Polymer Science and Technology, IBM Almaden Research Center, San Jose, California 95120-6099**Received January 14, 1994; Revised Manuscript Received August 12, 1994**

ABSTRACT: Poly(di-*n*-pentylsilane) has been previously reported to adopt a 7/3 helical conformation at room temperature. We have studied the solid state structure of a low molecular weight ($M_w = 46\,000$) sample and its dependence on temperature using wide angle X-ray diffraction, differential scanning calorimetry, and Raman spectroscopy. The results suggest that domains of two distinct structures are present, one having an all-trans conformation and the other a 7/3 helical conformation. The all-trans conformation was observed (even at room temperature) in samples cooled previously to $-15\text{ }^\circ\text{C}$. Characteristic resonance enhancement of certain Raman vibrations is observed for the planar zigzag polymorph. The all-trans material converts to the 7/3 helical structure at $35\text{ }^\circ\text{C}$ and subsequently undergoes an order/disorder transformation at about $56\text{ }^\circ\text{C}$.

Introduction

Poly(di-*n*-alkylsilanes), having the empirical formula $-(\text{SiRR}')_n-$, are silicon backbone polymers with alkyl (R, R') side chains. These polymers form a group of σ -conjugated materials. The extensive delocalization of σ electrons along the chain causes the electronic behavior, manifested in their UV absorption characteristics, to be closely coupled with the backbone conformation. This in turn is influenced by the nature of the alkyl side chains and the solid state molecular packing.

Potential applications for polysilanes arise from their excellent thermal and mechanical properties, coupled with their unusual and interesting UV absorption characteristics and nonlinear absorption properties. They can be used as thermal β -SiC ceramic precursors, as impregnating agents for strengthening ceramics, and as nondispersive photoconductors for photocopying applications. Other applications include their use as UV radiation sensitive materials for microlithography, as photoinitiators for vinyl polymerization, and for nonlinear optical applications.

Symmetrically-substituted alkyl polysilanes exhibit both reversible thermochromic¹ and piezochromic^{2,3} transitions, which involve changes in the conformation and packing of the polymer molecules.

Poly(di-*n*-hexylsilane), PdnHS, in which two hexyl side chains are attached to each silicon atom, has an optical absorption at $\sim 373\text{ nm}$ at room temperature. Above its structural transition temperature of $41\text{ }^\circ\text{C}$, the absorption blue-shifts to 313 nm and a concurrent change from an all-trans backbone conformation to a disordered conformation occurs. Polarized absorption spectra⁴ of a rubbed-oriented film of PdnHS show an energy shift in the absorption peak from 366 to 312 nm , indicating a decrease in the σ delocalization along the silicon backbone as the polymer disorders. Similar results have been observed⁵ for di-*n*-heptyl and di-*n*-octyl polysilanes which show X-ray diffraction patterns⁶ similar to that of PdnHS.

Poly(di-*n*-pentylsilane), PdnPS, on the other hand, has been previously reported⁷ to absorb at 313 nm at room temperature. The absorption peak does not change with temperature, although the polymer has a structural dis-

ordering transition at $76\text{ }^\circ\text{C}$. This suggests that the thermal transition in this polymer primarily involves a change in the packing of the molecules but not in the conformation of the silicon backbone. The piezochromic behavior of the polysilanes also involves backbone conformational changes. Application of moderate pressure causes PdnPS to absorb at 360 nm as the polymer adopts an all-trans conformation.^{2,3}

A series of symmetric and asymmetric poly(*n*-alkylsilanes) has been previously investigated^{6,8} at ambient and elevated temperatures to assess their crystalline conformations and solid state molecular packing. In the ordered, crystalline phases, three main backbone conformations have been found. The all-trans, planar zigzag conformation is observed in dimethyl,^{9,10} diethyl, di-*n*-propyl,¹¹ di-*n*-hexyl,^{5,12-15} di-*n*-heptyl, and di-*n*-octyl^{5,6,8} substituted polysilanes. The 7/3 helical conformation is observed in di-*n*-butyl¹³ and di-*n*-pentyl^{6-8,13,16} polysilanes. On the basis of NMR and UV evidence, poly(di-*n*-butylsilane) has also been reported¹⁷ to form a planar zigzag phase when precipitated at very low temperatures ($-78\text{ }^\circ\text{C}$). Structural ordering, however, was insufficient to give X-ray diffraction characteristic of the all-trans conformation. Polymers having nonyl or longer side chains adopt a TGTG' conformation.^{6,8}

Molecular modeling calculations^{18,19} show that both the 7/3 helical and planar zigzag conformations are low-energy conformations for polysilanes, with the helical form being slightly lower in energy. Intermolecular interactions may be responsible for the planar zigzag backbone in the longer side chain homologues. The adoption of an all-trans conformation in the shorter side chain polymers (methyl to propyl) has been attributed to electronic interactions within the silicon backbone.¹⁰ Recent energy calculations⁹ on poly(dimethylsilane), however, attribute the trans backbone to more efficient packing of the molecules in the all-trans conformation than would be possible for helical molecules. The TGTG' conformation has also been found by conformational calculations¹⁸ to be energetically feasible.

Further studies of the structure of PdnPS and its dependence on temperature and thermal treatment using X-ray diffraction, differential scanning calorimetry, and Raman spectroscopy are reported here. While PdnPS was

* Abstract published in *Advance ACS Abstracts*, October 1, 1994.

previously found^{6-8,13,16} to adopt a 7/3 helical backbone conformation at room temperature, an all-trans polymorph has now been observed at room temperature.

Experimental Section

X-ray Diffraction. As determined by gel permeation chromatography (GPC), the material used for this study was a relatively low molecular weight sample (M_w of $\sim 46 \times 10^3$) compared to the high molecular weight sample (M_w of $\sim 1 \times 10^6$) used previously.⁷ Fibers, from different pieces of the same material, were drawn on a TekStir hot stage and allowed to cool slowly to room temperature. The fiber samples were further cooled overnight in a refrigerator (at about -15°C) before the diffraction pictures were taken. These cooled samples will be referred to as the low-temperature ordered (LTO) material. Diffraction patterns at room and elevated temperatures were recorded on flat photographic film (Kodak DEF 5) using an evacuated Warhus camera. The camera is equipped with accessories for high-temperature operation. Temperature control was achieved by cycling the Omega Model 49 heater control to the desired temperature. A temperature stability of $\pm 0.3^\circ\text{C}$ was achieved. Fiber diffraction patterns were obtained using nickel-filtered Cu K α X-rays. Exposure times varied from 6 to 8 h.

Real-time WAXD studies of conformational changes were carried out using a rotating anode generator and a four-circle goniometer of the type commonly used for single crystal diffraction work. Most importantly, the diffraction patterns were captured digitally using a noncommercial area detector. The two-dimensional detector is a multiwire proportional chamber (MWPC), with a nominal working area of 250×250 mm and an effective pixel size of 1 mm (in the anode wire direction) \times 2 mm (anode wire spacing). In normal operation, the detector contains a 90% Xe–10% CO₂ mixture at atmospheric pressure and operates at a voltage of 2600–2700 V. The full width at half-maximum (FWHM) resolution in the anode delay line direction (perpendicular to the anode wires) is ~ 1.6 mm, while the FWHM resolution in the cathode delay line direction (parallel to the anode wires) is ~ 1.1 mm.

Sample-to-detector distances of 233, 237, and 270 mm (used respectively at detector angles of 0, 10, and 30°) were used. With the detector position at 10° , it was possible to observe the equatorial and near-meridional reflections simultaneously as the temperature was changed. At a position of 30° , meridional reflections out to less than 2 \AA could be observed.

The goniometer (Huber Model 408) provided three arcs to adjust the crystal orientation to bring any desired set of planes into diffracting position. The fiber was glued to a specially-designed wire loop with rubber cement to maintain it under slight tension. The wire loop was inserted into the goniometer head. Alignment of the fiber was achieved by observing the fiber through the telescope and making translational adjustments until its apparent center remained stationary as the sample was rotated.

The cooling system consisted of an FTS Systems Model XR-85-1 air jet cooler which directs a stream of dried, filtered, and cooled nitrogen onto the sample. Low-temperature diffraction studies were obtained by cooling the sample from room temperature to about -15°C . The sample was held at this temperature, and the diffraction patterns were recorded every 30 min until a change in the detector image, and hence a change in crystalline phase, was evident.

High temperature was achieved by blowing heated nitrogen onto the fiber sample. The goniometer head and the sample were enclosed in a sheet of Mylar to enhance temperature stability. Temperature was determined using a thermocouple positioned as near as possible to the specimen. Diffraction data were taken as the sample was heated slowly from -15 to about $+100^\circ\text{C}$ (total time of 3 h). Data were recorded at 2 deg intervals.

The Rigaku RU-200 X-ray generator was operated at 50 kV and 150 mA. The X-rays from the copper anode were monochromatized using a graphite monochromator. Exposure times of 20–60 s were sufficient to obtain the required X-ray data.

Calorimetry. The structural transition temperatures and the enthalpies of transition for the different phases were determined from differential scanning calorimetry (DSC). The thermal

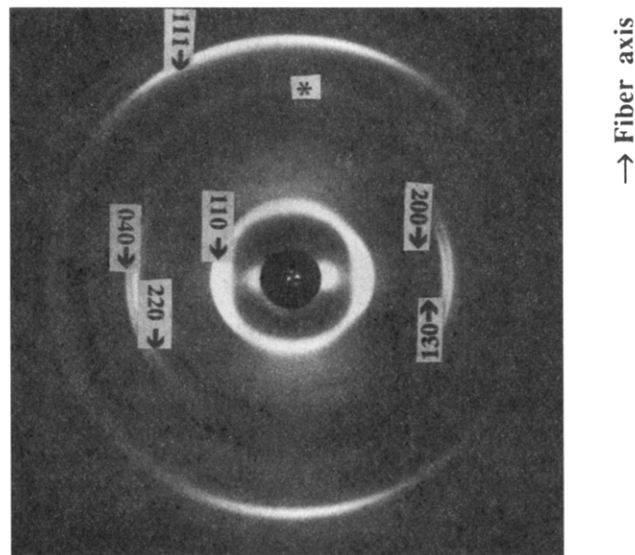


Figure 1. PdnPS at room temperature (all-trans).

measurements were made with a computer-controlled General V4.1C DuPont 2100 differential scanning calorimeter. Heating and cooling rates of $5^\circ\text{C}/\text{min}$ were utilized over a temperature range from -50 to about $+90^\circ\text{C}$.

Spectroscopy. Raman spectra were recorded using a Jobin-Yvon HG-2S double monochromator equipped with concave holographic gratings and a spatial filter to enhance stray light rejection. Because of its high sensitivity and low dark count, a cooled RCA 31034A-02 photomultiplier tube (operating at -1500 V) was used to detect the scattered photons. Laser excitation was provided by the 488 nm line of a Spectra Physics 2020 argon ion laser in the 90° scattering geometry. Excitation powers were typically 100–300 mW. Entrance and exit slits were set to give a spectral resolution of 2 cm^{-1} . All data were collected and processed digitally by a Nicolet 1180 data system. The Raman spectra shown have not been filtered or smoothed in any way. Variable temperature measurements were made in a vertical Harney-Miller cell especially constructed for operation in the -150 to $+150^\circ\text{C}$ range. With this cell, the sample could be maintained within ± 1 deg of the desired temperature.

One sample was characterized in the unoriented form before and after temperature cycling. The other samples were prepared in the same manner as the X-ray samples (oriented by drawing on a hot stage). Samples were placed in glass capillary tubes for Raman measurements.

Results

Diffraction. In the previous studies⁷ of PdnPS, the room temperature diffraction pattern was taken after orienting the sample at room temperature. In this work, the fiber sample was cooled to -15°C before the diffraction pictures were taken at room temperature. The diffraction pattern (Figure 1) for this moderately oriented sample of low-temperature ordered (LTO) material shows a composite pattern with characteristics of diffraction patterns from di-*n*-alkyl polysilanes having the silicon backbone in trans-planar and 7/3 helical conformations. The composite diffraction pattern is, however, dominated by reflections from the all-trans polymorphic form. The intense, near-meridional reflection at a d spacing of 3.78 \AA is a smear of a pair of (111) reflections, similar to that observed^{12,14} in PdnHS. When the characteristic reflections from the helical form were ignored, the remaining reflections were indexed by a metrically orthorhombic unit cell with dimensions $a = 13.7 \text{ \AA}$, $b = 21.4 \text{ \AA}$, and $c = 4.0 \text{ \AA}$. The layer line spacing of 4.0 \AA is consistent with an all-trans, planar zigzag backbone conformation. It is not entirely surprising that the all-trans polymorph is found for PdnPS since a piezochromic response, with an apparent change

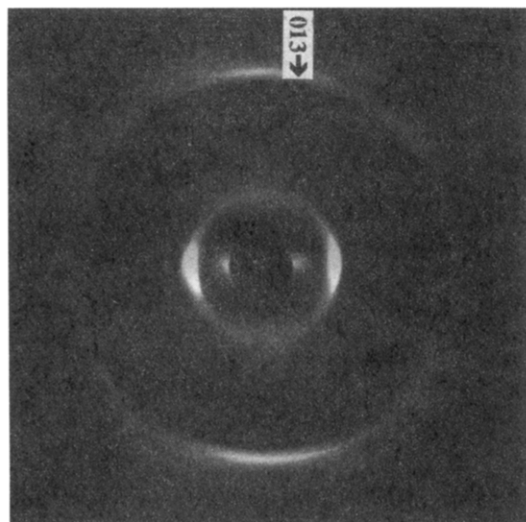


Figure 2. PdnPS at 35 °C (helix).

in the backbone conformation from the low-energy 7/3 helix to an all-trans conformation, has been reported previously.^{2,3} However, the existence of an all-trans polymorph under ambient conditions was unexpected. We denote this new polymorph of PdnPS as form III.

The least squares refinement of the unit cell parameters gave average discrepancies in the d spacings (Δd) and the diffraction angles ($\Delta 2\theta$) of 0.02 Å and 0.04°, respectively. Based on two molecules per unit cell, the X-ray density calculated from the unit cell parameters gives a value of 0.96 g/cm³. This compares with a value of 1.00 g/cm³ for the X-ray density of PdnHS¹² for a cell having dimensions $a = 13.8$ Å, $b = 23.9$ Å, and $c = 3.99$ Å.

The all-trans polymorph undergoes a phase transition at 35 °C. Peaks from the all-trans phase decrease in intensity while those from the helical phase increase. Above 35 °C, the diffraction pattern (Figure 2) is similar to that obtained⁷ previously for the helical form of PdnPS (form I) at room temperature. The reflections on the first and second layer lines, although discernible, were not as distinct as observed previously. The intense zero layer reflections, which relate to the interchain backbone spacing, were indexed as (100) reflections. A strong near-meridional reflection appeared on the third layer line at a d spacing of 4.52 Å (as compared to 4.49 Å in the previous⁷ sample) and was indexed as (013). The layer line spacing of 13.9 Å is consistent with a 7/3 helix. The Bragg reflections were indexed by a metrically monoclinic unit cell with dimensions $a = 13.9$ Å, $b = 24.5$ Å, $c = 13.9$ Å, and $\gamma = 120^\circ$. The average Δd and $\Delta 2\theta$ were calculated to be 0.04 Å and 0.04°. The Bragg reflections from the previous sample were also indexed⁶ by a metrically monoclinic unit cell with dimensions $a = 13.8$ Å, $b = 23.8$ Å, $c = 13.9$ Å, and $\gamma = 120^\circ$. The average Δd and $\Delta 2\theta$ values were 0.01 Å and 0.03°. The differences in these cells are within experimental error. The measured d spacings are slightly different in the two samples, although both can be indexed adequately by a metrically monoclinic lattice. More important is that different sets of reflections are observed. Those with corresponding d spacings have the same indices, but many are observed in only one pattern or the other. The difference in molecular weight of the two samples, and also the effect of temperature, may account for the differences in the observed d spacings. Table 1 shows the WAXD data for both the all-trans and helical polymorphic forms of PdnPS measured from the X-ray film.

Further insight into the structural changes occurring at the transition was gained from X-ray diffractometry

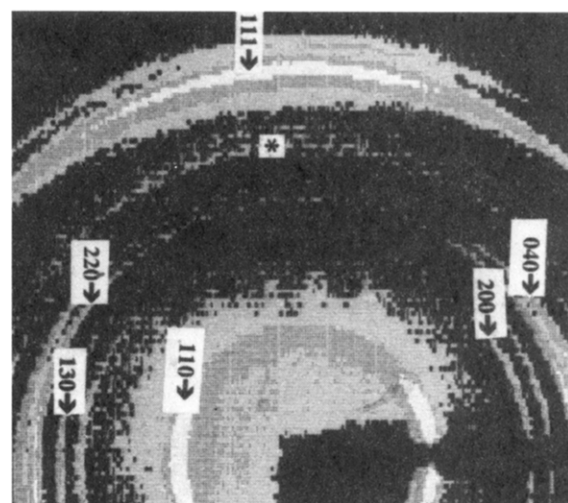


Figure 3. Detector image of PdnPS at 30 °C (trans) (detector angle = 10°; * indicates reflection from helical phase).

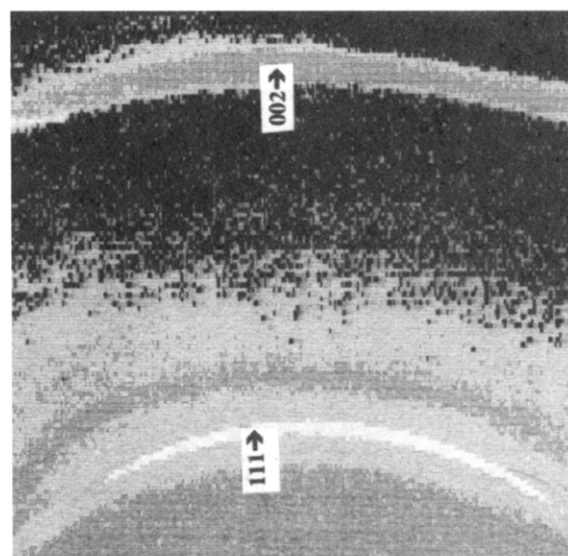


Figure 4. Detector image of PdnPS at 30 °C (detector angle = 30°).

Table 1

<i>hkl</i>	d_{obs} (Å)	d_{calc} (Å)	<i>hkl</i>	d_{obs} (Å)	d_{calc} (Å)
(i) WAXD Data for PdnPS at Room Temperature (All-Trans Polymorph)					
110	11.50	11.53	310	4.48	4.47
200	6.83	6.85	150	4.07	4.08
130	6.30	6.32	111	3.78	3.78
220	5.70	5.76	121	3.61	3.61
040	5.34	5.34	360	2.81	2.81
140	4.99	4.98	450	2.67	2.67
(ii) Data for PdnPS at 35 °C (7/3 Helical Polymorph)					
100	11.88	12.02	210	5.14	5.15
110	8.90	8.74	131	4.78	4.77
030	7.06	7.07	2, -3, 2	4.72	4.72
2, -3, 0	6.43	6.43	013	4.52	4.52
(iii) Data for PdnPS (Previous Sample) at 25 °C ^{6,8}					
100	11.83	11.92	013	4.49	4.49
110	8.53	8.62	2, -4, 2	4.30	4.30
2, -1, 0	6.67	6.68	050	4.13	4.13
200	5.96	5.96	132	4.04	4.04
130	4.98	4.97	1, -3, 3	3.98	3.98
131	4.65	4.68	060	3.44	3.44

studies using a four-circle single crystal goniometer and area detector. Figures 3–7 show the detector images of the sample (fiber axis vertical) through the structural transitions. The composite nature of the room tempera-

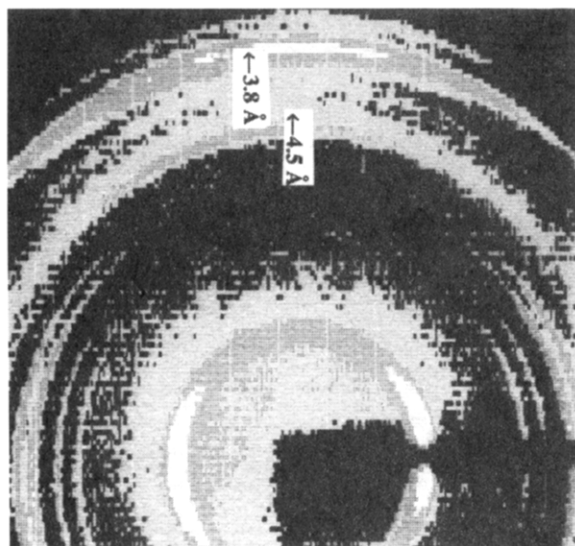


Figure 5. Detector image of PdnPS at 32 °C (detector angle = 10°).

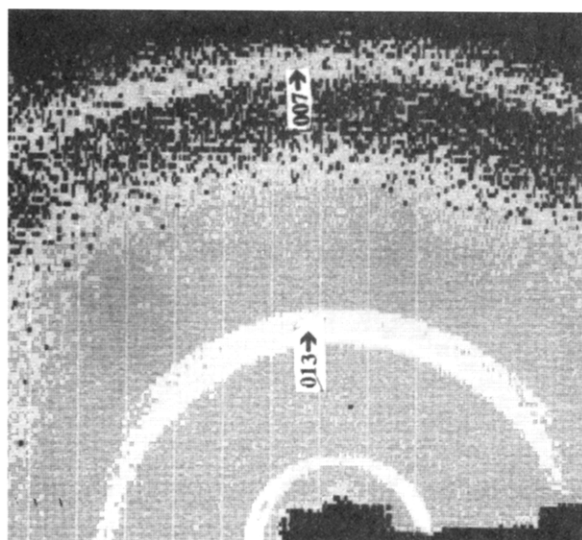


Figure 6. Detector image of PdnPS at 35 °C (helical) (detector angle = 30°).

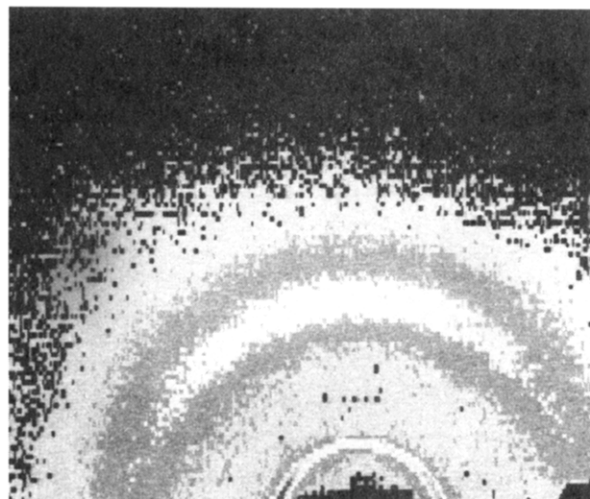


Figure 7. Detector image of PdnPS at 100 °C (detector angle = 30°).

ture diffraction pattern is evident in the detector image shown in Figure 3. The 002 reflection (at $d = 2.0$ Å) evident in the pattern taken at a detector angle of 30° (Figure 4)

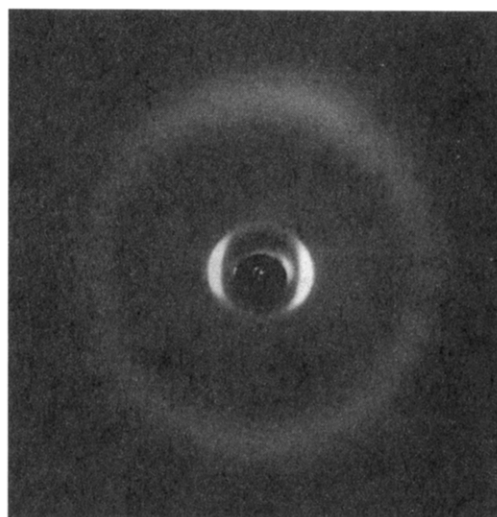


Figure 8. PdnPS at 100 °C.

is characteristic for polymers having an all-trans silicon backbone. At 32 °C, the digitized image (Figure 5) clearly shows two near-meridional reflections at d spacings of 3.8 and 4.5 Å, indicating that the PdnPS sample contains both all-trans and 7/3 helical forms, as also observed in the film diffraction patterns. The 3.8 Å reflection, indexed as (111), is the reflection observed for the all-trans polymorphic form.

At 35 °C, the near-meridional reflections (Figure 5) merge into one strong reflection at $d = 4.5$ Å (Figure 6). This (013) reflection was found to lie on the third layer line on the photographic X-ray pattern. This 4.5 Å reflection on the third layer line and the 007 reflection at $d = 1.97$ Å confirm the 7/3 helical conformation. The shift of $\sim 1^\circ$ (2θ) from $d = 2.0$ Å [(002) reflection from the all-trans material] to the 1.97 Å d spacing of the (007) reflection of a 7/3 helix confirms the change from an all-trans to a 7/3 helical conformation.

Similar to PdnHS and other polysilanes previously studied, at 100 °C most of the sharp reflections from the ordered 7/3 helix of this sample of PdnPS smear out into an amorphous halo, as seen in Figures 7 and 8. The amorphous halo centered at ~ 4 Å indicates a lack of three-dimensional ordering as a result of intramolecular disordering of the side chains. The (007) reflection at 1.97 Å observed in Figure 6 disappeared between 60 and 65 °C (Figure 7), indicating disordering of the helical conformation and loss of registry between molecules (parallel to the chain axes).

Hysteresis was observed upon cooling the sample back to room temperature. As the sample cooled to ~ 40 °C, the helical diffraction pattern became evident and persisted. To restore the all-trans conformation, it was necessary to cool the sample again to -15 °C. Analysis of the real-time diffraction data shows that at -15 °C, the all-trans structure develops within about 7 h. Figure 9 shows slices through the detector images of the helical conformation at time $t = 0$ h and the restoration of the all-trans conformation at $t = 6$ –7 h. The transformation is evident from the appearance of the sharp peak at $\sim 16^\circ$ (2θ) which corresponds to the 5.7 Å reflection measured on the X-ray film for the all-trans polymorph.

Thermal Analysis. Figure 10 shows the DSC thermogram of LTO PdnPS initially in form III obtained at a heating rate of 5 °C/min. The thermogram shows two endothermic peaks at ~ 35 and ~ 56 °C. The DSC results are in good agreement with the X-ray results which showed a transition at 35 °C, corresponding to a change from mixed

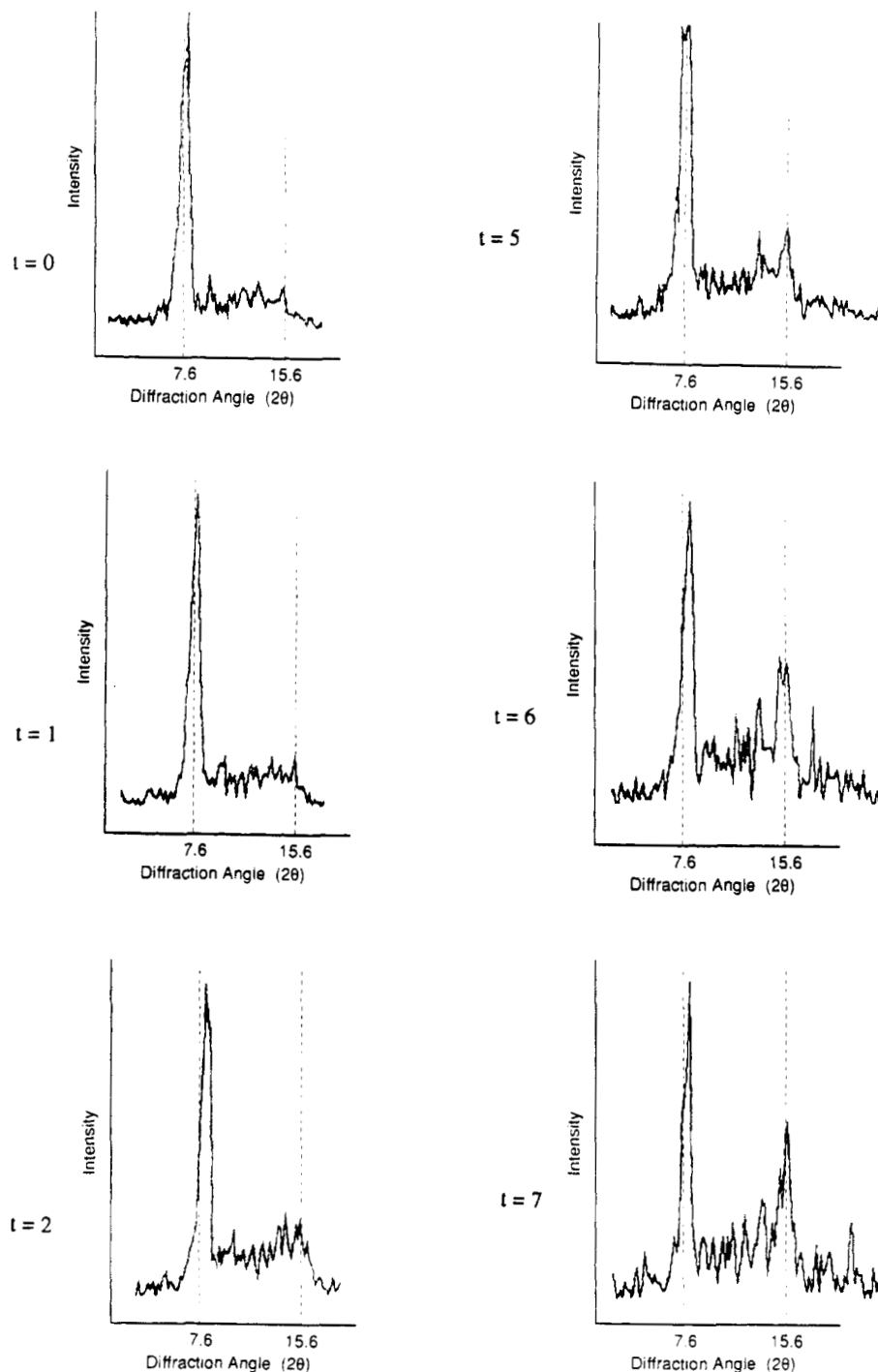


Figure 9. Diffraction peaks of detector image of PdnPS at -15°C .

phase material to one having a 7/3 helical structure, and a structural disordering transition at $\sim 60^{\circ}\text{C}$.

Without knowledge of the fraction of the material that is in form III, the heat of the transformation at 35°C cannot be determined. The heat for the 56°C peak (form I to II) is ~ 0.68 kcal/mol. Schilling et al.¹³ previously reported a solid state disordering transition in PdnPS at 70°C with an enthalpy of transformation from form I to II of ~ 0.51 kcal/mol. Miller et al. also observed this transition at 74°C .⁷ The lower temperature and different heat of transformation observed here could be due to molecular weight effects, crystallinity, heating rate, or thermal history.

Spectroscopy. Raman spectra were taken in the region from 800 to 50 cm^{-1} , focusing on the vibrational modes associated with the silicon main chain. The bending vibrations [$\delta(\text{Si-Si-Si})$, $\delta(\text{Si-Si-C})$, etc.] and lattice modes fall below 350 cm^{-1} . The Si-Si stretches are generally

found in the region from 350 to 500 cm^{-1} , while Si-C stretches occur above 500 cm^{-1} .

The room temperature (25°C) spectrum of a virgin sample (synthesized, purified, and then obtained as a solid by freeze-drying), shown in Figure 11 (curve A), indicates the presence of the planar zig-zag conformation. In previous work on PdnHS,^{14,20} the strong band at 689 cm^{-1} was shown to correspond to the symmetric Si-C stretching mode of the ordered planar backbone. Hence, the 689 cm^{-1} band may be used as the fingerprint of the planar zigzag structure in the poly(di-*n*-alkylsilanes). Resonance enhancement of the vibrations associated with the σ -conjugated silicon backbone, best illustrated by the Si-C stretch at 689 cm^{-1} , occurs only for the planar zigzag conformation.

When the sample was heated through the transition at $\sim 35^{\circ}\text{C}$, the Raman spectrum changed dramatically (as seen in Figure 11, curve B), reflecting the conformational

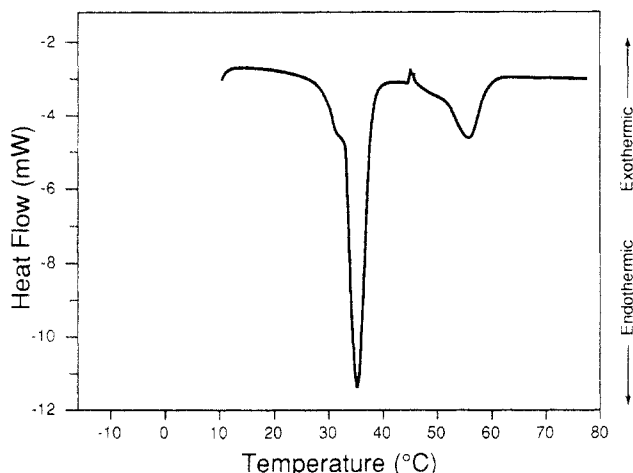


Figure 10. DSC thermogram of PdnPS (heating rate = 5 °C/min).

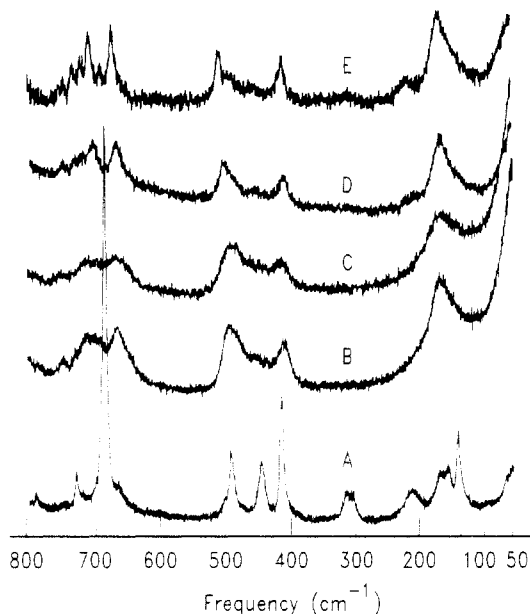


Figure 11. Raman spectra of PdnPS from 800 to 50 cm^{-1} : virgin material (A) at 25 °C, (B) at 50 °C, (C) at 90 °C, (D) upon cooling to 25 °C, (E) at -50 °C.

changes in the silicon backbone. The WAXD results show that the PdnPS exists as a 7/3 helix at these temperatures. The peaks which have been lost on heating the sample through its 35 °C transition (138, 214, 310, 444, and 689 cm^{-1}) may be confidently attributed to vibrations involving the planar zigzag silicon backbone. The remaining peaks may be assigned to the helical form of PdnPS. Some of these bands are slightly shifted in frequency and all spectral features are much broader in the 50 °C spectrum.

In comparing the original room temperature spectrum (curve A) with the 50 °C spectrum (curve B), one concludes that at room temperature the virgin sample contains a mixture of both the all-trans and the helical backbone conformations. The X-ray results concur with the simultaneous existence of the two polymorphs. After heating through the 35 °C transition, most of the all-trans sequences are lost.

On going from the 7/3 helix (50 °C, Figure 11, curve B) to the disordered form (90 °C, Figure 11, curve C), the spectrum does not change very much; only a slight broadening of peaks is observed. X-ray patterns indicate that the chains form a disordered two-dimensional hexagonal array. The broadening observed in the vibrational spectrum is due to the introduction of defects in the silicon main chain conformation.

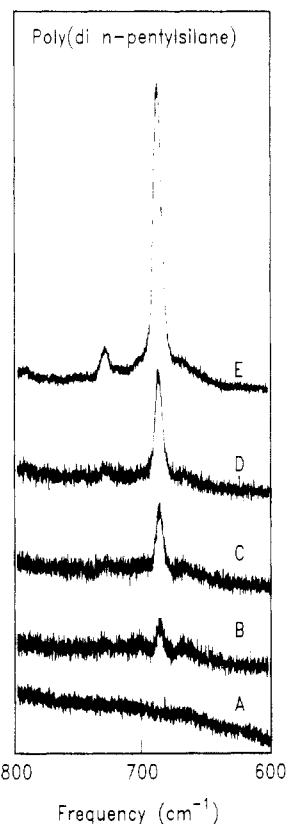


Figure 12. Si-C stretching region of the Raman spectra of PdnPS from 800 to 600 cm^{-1} as a function of time. The material in curve A is in the 7/3 helical form at room temperature. The sample has been held at -15 °C for 5 h in curve B, 6 h in curve C, and 7 h in curve D. In curve E the sample was held at -15 °C for 7 h, was allowed to warm overnight to room temperature (25 °C), and then was held at -15 °C for another 7 h.

Table 2. Raman Spectral Assignments

cm^{-1}	helix	planar zigzag
138		$\delta(\text{Si-Si-Si}) +$ lattice vibrations
154, 170 > 161	$\delta(\text{Si-Si-Si}) +$ lattice vibrations	
214		$\delta(\text{Si-Si-Si})$
304/314		$\delta(\text{Si-Si-Si})$
414	$V_s(\text{Si-Si})$	
444		$V_s(\text{Si-Si})$
492, 502	$V_s(\text{Si-Si})$	$V_s(\text{Si-Si})$
668	$V_s(\text{Si-C})$	
689		$V_s(\text{Si-C})$
714 (707)	$V_s(\text{Si-C})$	
730		$V_s(\text{Si-C})$
750	$V_s(\text{Si-C})$	
792		

Shown in Table 2 are the Raman spectral assignments based on previous assignments in PdnPS² and PdnHS,^{2,14,20} and the identification of modes originating from the two different silicon main chain conformations.

After the sample was cooled to room temperature, the spectrum was measured again. One sees from Figure 11 (curve D) that the ordered helical structure is formed. Because the disordered to ordered helical transition was shown by DSC to require an undercooling of approximately 20 °C, the sample was further cooled to -50 °C with the intention of converting the ordered helical material to planar zigzag. As is clear from Figure 11 (curve E), most of the material remained frozen in the disordered form. (Some planar zigzag sequences have formed, as seen from the presence of weak all-trans bands.) The maximum conversion to the all-trans conformation was achieved by holding the sample at -15 °C for approximately 7 h. Figure 12 illustrates this transition by following the increase in

intensity of the 689 cm^{-1} band as a function of time. The transition to the planar zigzag conformation was demonstrated in similar experiments using DSC and WAXD. The endotherm characteristic of formation of the all-trans species is restored with the low-temperature treatment. These results indicate that the transformation to the planar zigzag form is a kinetically limited process. X-ray patterns obtained from some samples, however, over a period of several weeks indicate that the 7/3 helical and planar zigzag phases are stable at room temperature for long periods. In the DSC data, the amount of material transforming from the 7/3 helix to the disordered phase is the same whether planar zigzag was previously present or not.

Discussion

Conformational calculations showed that the 7/3 helical conformation adopted^{7,16,17} by PdnPS was the preferred low-energy conformation for an isolated molecule. This suggests that the adoption of an all-trans conformation in PdnPS (and in PdnHS as well) results, in part, from intermolecular interactions.^{9,18,19} One may interpret the transition from form III to I at 35 °C as resulting from a partial breakdown of these intermolecular interactions, allowing the polymer to return to a lower (intramolecular) energy conformation. Low-temperature DSC studies of the 35 °C transition show that after heating the LTO material once through the 35 °C transition, the sample must be held at -15 °C (an undercooling of approximately 50 °C) for 7 h before the transition can be measured again.

Neither the transition temperature nor the enthalpy of the transition at 56 °C appears to depend on the amount of all-trans material in the sample (as judged by holding at 45 °C for various lengths of time). Planar zigzag material apparently does not form at temperatures above the 35 °C transition, and any that might have been present initially (by previous cooling to -15 °C) is lost entirely at the 35 °C transition. Upon cooling (assuming sufficient undercooling for a long enough time), the amount of all-trans material formed is similar to that observed originally. Some helical phase material was always present whenever the polymer was ordered.

It is interesting to note that in the samples of PdnPS studied here, two distinct structures seem to coexist. Vibrations due to both populations are observed in the Raman spectra. A possible explanation for the presence of these structures may be associated with the molecular weight of the material. While there was no evidence (in the GPC data) of a bimodal molecular weight distribution in this sample, the molecular weight was much lower than that of the material used previously and the distribution was rather broad. In this molecular weight range, both helical and planar zigzag forms may be energetically comparable, with the former becoming more dominant in higher molecular weight material. This might be analogous to the highest molecular weight polyethylene, where the degree of crystallinity is reduced, apparently because kinetic factors limit the crystallization process. Similarly in the polysilanes, a high molecular weight could limit the ability of the material to exclude defects or to otherwise optimize the chain packing in the crystalline regions. For this or other reasons, the planar zigzag conformation may not be favored except in relatively short chains. While the application of pressure may be able to cause the transition to the planar zigzag form even in the higher molecular weight material, lowering the temperature only converts lower molecular weight material to this form after several hours.

Conclusions

Properly prepared samples of low molecular weight PdnPS can contain both the helical (form I) and all-trans (form III) polymorphs at room temperature. Vibrations involving the silicon backbone of the planar zigzag polymorph are resonantly enhanced and are easily used to identify this polymorph. On heating, the all-trans polymorph undergoes a transition to a helix at 35 °C. The reverse transition (from the helical to the all-trans form) is kinetically limited, requiring about 7 h at -15 °C (an undercooling of about 50 °C). The 7/3 helical polymorph is likewise stable at room temperature. It undergoes a transition to a disordered structure near 60 °C. An undercooling of approximately 20 °C is required to cause the transition back to the ordered helical form.

The unit cell for form III is metrically orthorhombic with dimensions $a = 13.7 \text{ \AA}$, $b = 21.4 \text{ \AA}$, and $c = 4.0 \text{ \AA}$. This compares with form I which has an ordered 7/3 helical chain conformation with a repeat distance of 13.9 Å. The unit cell for form I is metrically monoclinic with dimensions $a = 13.9 \text{ \AA}$, $b = 24.5 \text{ \AA}$, $c = 13.9 \text{ \AA}$, and $\gamma = 120^\circ$. At ~60 °C, form II is observed. The X-ray diffraction data show that the polymer molecules pack in a columnar hexagonal arrangement with cell dimensions $a = b = 14.3 \text{ \AA}$.

Acknowledgment. We thank Professor Robert Kretsinger and Dr. Ron Chandross of the University of Virginia for allowing us to use the X-ray facility at the Physics Department. We gratefully acknowledge Hoa Truong of the IBM Almaden Research Center for performing the low-temperature DSC measurements. We also thank Richard Siemens also of IBM Almaden Research Center for help in designing the DSC experiments.

References and Notes

- Miller, R. D.; Hofer, D.; Rabolt, J. F.; Fickes, G. N. *J. Am. Chem. Soc.* **1985**, *107*, 2172.
- Schilling, F. C.; Bovey, F. A.; Davis, D. D.; Lovinger, A. J.; Macgregor, R. B., Jr.; Walsh, C. A.; Zeigler, J. M. *Macromolecules* **1989**, *22*, 4645.
- Song, K.; Miller, R. D.; Wallraff, G. M.; Rabolt, J. F. *Macromolecules* **1991**, *24*, 4084.
- Tachibana, H.; Matsumoto, M.; Tokura, Y. *Macromolecules* **1993**, *26*, 2520.
- Rabolt, J. F.; Hofer, D.; Miller, R. D.; Fickes, G. N. *Macromolecules* **1986**, *19*, 611.
- Karikari, E. K.; Farmer, B. L.; Miller, R. D.; Rabolt, J. F. *Macromolecules* **1993**, *26*, 3937.
- Miller, R. D.; Farmer, B. L.; Fleming, W.; Sooriyakumaran, R.; Rabolt, J. F. *J. Am. Chem. Soc.* **1987**, *109*, 2509.
- Karikari, E. K.; Farmer, B. L.; Miller, R. D.; Rabolt, J. F. *Polym. Prepr. (Am. Chem. Soc., Div. Polym. Chem.)* **1991**, *31*, 290.
- Patnaik, S. S.; Farmer, B. L. *Polymer* **1992**, *33*, 5127.
- Lovinger, A. J.; Davis, D. D.; Schilling, F. C.; Padden, F. J.; Bovey, F. A.; Zeigler, J. M. *Macromolecules* **1991**, *24*, 132.
- Lovinger, A. J.; Davis, D. D.; Schilling, F. C.; Bovey, F. A.; Zeigler, J. M. *Polym. Commun.* **1989**, *30*, 356.
- Patnaik, S. S.; Farmer, B. L. *Polymer* **1992**, *33*, 4443.
- Schilling, F. C.; Lovinger, A. J.; Zeigler, J. M.; Davis, D. D.; Bovey, F. A. *Macromolecules* **1989**, *22*, 3055.
- Kuzmany, H.; Rabolt, J. F.; Farmer, B. L.; Miller, R. D. *J. Chem. Phys.* **1986**, *85*, 7413.
- Lovinger, A. J.; Schilling, F. C.; Bovey, F. A.; Zeigler, J. M. *Macromolecules* **1986**, *19*, 2657.
- Farmer, B. L.; Rabolt, J. F.; Miller, R. D. *Macromolecules* **1987**, *20*, 1167.
- Walsh, C. A.; Schilling, F. C.; Lovinger, A. J.; Davis, D. D.; Bovey, F. A.; Zeigler, J. M. *Macromolecules* **1990**, *23*, 1742.
- Chapman, B. R.; Farmer, B. L. *Polym. Prepr. (Am. Chem. Soc., Div. Polym. Chem.)* **1990**, *31*, 288.
- Chapman, B. R.; Patnaik, S. S.; Farmer, B. L. *Polym. Prepr. (Am. Chem. Soc., Div. Polym. Chem.)* **1990**, *31*, 1265.